Photoluminescence and Electroluminescence of d^6 Metal−Organic Conjugated Oligomers: Correlation of Photophysics and Device Performance

Garry B. Cunningham, Yiting Li, Shengxia Liu, and Kirk S. Schanze*

Department of Chemistry, University of Florida, P.O. Box 117200, Gainesville, Florida 32611

Received: June 26, 2003; In Final Form: October 3, 2003

The photophysical and electroluminescent device properties of a series of d^6 transition metal complexes that feature an oligo(aryleneethynylene) (OAE) "ligand" have been investigated. The metals are coordinated η_2-to the OAE via a 2,2′-bipyridine moiety that is in the "core" of the oligomer, and the metals used are η_2-$Ir(ppy)_2^+$, η_2-$Ru(bpy)_2^{2+}$, and η_2-$Os(bpy)_2^{2+}$ (Ir-2, Ru-2, and Os-2, respectively, where ppy = 2-phenylpyridine and bpy = 2,2′-bipyridine). The photoluminescence spectra and excited-state decay parameters for the metal−OAEs indicate that at ambient temperature Ru-2 and Os-2 feature a lowest ^{3}MLCT excited state; however, in Ir-2 the lowest excited state is $^3\pi,\pi^*$ localized on the OAE. Electroluminescent (EL) devices that contain the metal−OAEs dispersed at 5 wt % in a poly(vinyl carbazole):2-(4-*tert*-butylphenyl)-5-(4-biphenylyl)-1,3,4-oxadiazole matrix exhibit electroluminescence at wavelengths that correlate well with the photoluminescence from the complexes in a rigid glass at low temperature. The EL efficiency of the devices varies in the order Ir-2 > Ru-2 ≫ Os-2. Factors that may contribute to the difference in EL efficiencies are discussed.

Introduction

There has been considerable recent interest in the optical and electronic properties of transition metal containing organic materials because of their potential for application in optical and electrooptical devices such as organic light emitting diodes (OLEDs), electrochromic, photovoltaic and photoconductive devices, and photorefractive optical elements.[1−9] The application for metal−organic materials which has received the greatest attention is OLEDs. In particular, since the finding by Thompson, Forrest, and co-workers that electron-to-photon quantum efficiencies (QE) approaching unity can be attained in OLEDs that contain organometallic iridium(III) complexes as the emitters,[2] much effort has been put into development of new phosphorescent compounds. The metal−organic based OLEDs display high QE due to their ability to harvest triplet excited states produced by electron−hole pair recombination.[1,2]

We are investigating the photophysics of π-conjugated systems featuring transition metals that interact strongly with the π-electron systems. In the course of this work we have examined poly(aryleneethynylene)s (PAEs) and oligo(aryleneethynylene)s (OAEs) that contain rhenium(I), ruthenium(II), and iridium(III) metal complexes.[10−12] The metal−organic PAEs and OAEs feature luminescent and long lifetime excited states having either triplet metal-to-ligand charge transfer (^{3}MLCT) or $^3\pi,\pi^*$ character. The ^{3}MLCT state involves charge transfer from the d^6 metal to the π-conjugated "ligand", whereas the $^3\pi,\pi^*$ state is localized on the π-electron system.

In the present investigation we compare the photophysics and electroluminescent device performance of a series of OAEs that contain d^6 complexes of Ir(III), Ru(II), and Os(II) (Ir-2, Ru-2, and Os-2).

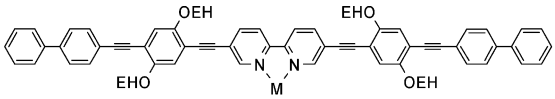

Ir-2 : M = $Ir(ppy)_2^+$ [PF_6^-] **Ru-2** : M = $Ru(bpy)_2^{2+}$ [PF_6^-]$_2$ **Os-2** : M = $Os(bpy)_2^{2+}$ [PF_6^-]$_2$

EH = 2-ethylhexyl, ppy = 2-phenylpyridine, bpy = 2,2'-bipyridine

The OAE ligand was selected for this study on the basis of previous investigations that demonstrated that the 8-ring oligomer is sufficiently long so that it accurately models the π-electron system of the analogous polymer. Investigation of the photophysics of the series of OAEs allows us to assign the lowest excited state as arising from ^{3}MLCT or OAE-based $^3\pi,\pi^*$. The photophysical properties of the metal−OAEs are then correlated with their performance in electroluminescent devices. The findings of this study reveal that all of the metal−OAEs feature red PL and EL at wavelengths ranging from 600 nm for Ir-2 complex to >850 nm in the near-infrared (near-IR) for the Os-2 system. Interestingly, we find that the electron-to-photon QE of the Ir-2 based EL device is the largest of the series. The photophysical data suggest that the higher QE of the Ir-2 based device arises due to the large spin−orbit coupling provided by the Ir(III) center, which enhances the probability of electrophosphorescence from the OAE-based $^3\pi,\pi^*$ state.

Results and Discussion

Optical and photophysical parameters for the metal−OAEs obtained in 2-methyltetrahydrofuran (MTHF) are collected in Table 1. The first column lists maxima and molar absorptivity values (λ_{max} and ϵ_{max}, respectively) for the near-UV and visible absorption bands of the metal−OAEs. All three complexes feature very similar absorption spectra in the near-UV and visible spectral regions, with an intense band at $\lambda_{max} \approx 340$ nm along with a less intense transition in the visible at $\lambda_{max} \approx 450$ nm. Because the absorption of the three metal−OAEs is quite

* To whom correspondence should be addressed. Tel: 352-392-9133. Fax: 352-392-2395. E-mail: kschanze@chem.ufl.edu.

10.1021/jp0358228 CCC: $25.00
Published on Web 10/30/2003

TABLE 1: Optical Properties of Metal−OAEs[a]

		photoluminescence								electroluminescence	
complex	absorption UV−vis abs λ_{max}/nm (ϵ_{max}/mM^{-1} cm^{-1})	λ_{max}/nm (E_{max}/eV) 298 K	λ_{max}/nm 80 K	τ_{em}/ns 298 K	ϕ_{em}[b]	k_r/ 10^4 s^{-1} [c]	k_{nr}/ 10^6 s^{-1} [c]	E_{MLCT}/ eV[d]	$E_{Triplet}$/ eV[e]	λ_{max}/ nm	ϕ_{EL}[f]
Ir-2	336 (69.1) 444 (52.5)	645 (1.92)	620	3300	0.026	0.79	0.29	1.9	1.9	593	0.012
Ru-2	342 (64.3) 458 (48.7)	701 (1.77)	658	706	0.034	4.4	1.3	1.8	1.9	644	0.0025
Os-2	354 (67.9) 459 (53.2) 550−740 (3)	848 (1.46)	787	32	0.00073	2.3	50	1.6	1.9	747	0.0003

[a] All measurements carried out in 2-methyltetrahydrofuran solvent (or solvent glass). [b] Quantum yields determined relative to $Ru(bpy)_3^{2+}$ in H_2O ($\phi_{em} = 0.055$). [c] Computed according to equations $k_r = \phi_{em}/\tau_{em}$ and $k_{nr} = 1/\tau_{em}$; assumes that the emitting excited state is reached with unit quantum yield. [d] Estimated according to the equation $E_{MLCT} = E_{1/2}{}^{ox}(\text{metal−OAE}) - E_{1/2}{}^{red}(\text{metal−OAE}) - \beta$, where $\beta = 0.5$ eV for Ir-2 and Ru-2 and 0.25 eV for Os-2, see refs 12, 14, 28, and 29. Estimated error is ± 0.1 eV. [e] From ref 10. [f] Maximum external EL quantum yield.

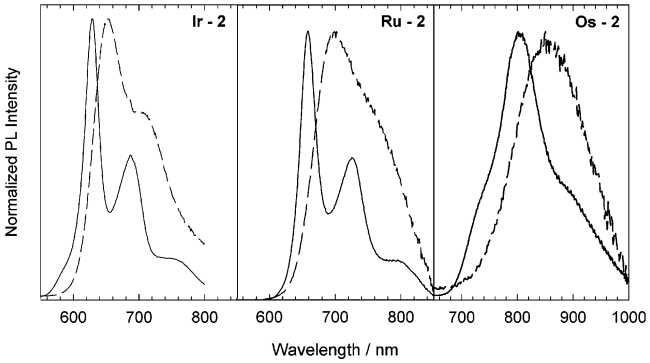

Figure 1. Photoluminescence spectra of metal−OAE complexes in 2-MTHF solution: (- - -) ambient temperature; (—) 80 K.

similar, it is evident that their primary absorption features arise from π,π^* transitions centered on the OAE. (The spin-allowed MLCT transitions, which typically have $\epsilon \approx 15\,000$ M^{-1} cm^{-1} are obscured by the more intense π,π^* bands.) An additional broad and relatively weak absorption band that extends from the tail of the low-energy π,π^* transition out to nearly 740 nm is seen in the spectrum Os-2. This weak transition is observed in other Os(II)−polypyridine complexes and has been previously assigned as arising from the spin-forbidden absorption to ^{3}MLCT.[13] In sum, the absorption of all three of the metal complex oligomers are very similar and the primary transitions are dominated by OAE-based π,π^* bands.

Prior to discussing the photophysical data on the metal−OAEs, it is important to note that in previous investigations of related systems we have demonstrated that the π-conjugated OAE "ligand" features a $^3\pi,\pi^*$ excited state with an energy of $\approx$1.9 eV (650 nm).[10] In addition to the $^3\pi,\pi^*$ state, the metal−OAEs are expected to feature energetically low-lying ^{3}MLCT states. The energy of the ^{3}MLCT state can be predicted on the basis of electrochemistry,[14] and as shown below, for the metal−OAEs the ^{3}MLCT manifold is in close energetic proximity to the $^3\pi,\pi^*$ state. Thus, the observed photophysics of the series of metal−OAEs is expected to emanate from one (or a combination of) these two excited-state manifolds.

Figure 1 illustrates PL spectra of the three metal−OAEs obtained in solution at ambient temperature and in a glass at 80 K (MTHF solvent) and emission band maxima are listed in Table 1. There are a number of features that become significant when one inspects the PL data. First, at both ambient temperature and in the 80 K glass, the emission red shifts considerably across the series in the order $\lambda_{max}{}^{em}$ Ir-2 < Ru-2 < Os-2. The emission maximum for Ir-2 corresponds very closely to the energy of the OAE-based $^3\pi,\pi^*$ state, whereas $\lambda_{max}{}^{em}$ for Ru-2 and Os-2 is at a lower energy than the $^3\pi,\pi^*$ state. This feature suggests that the nature of the photoluminescent excited state may change across the series. The second noteworthy feature concerns the vibronic structure in the PL spectra. Specifically, in the 80 K MTHF solvent glass, Ir-2 and Ru-2 exhibit a well-resolved vibronic progression, but Os-2 does not. In the ambient temperature spectra, only Ir-2 features a discernible vibronic progression. In previous studies of d^6 transition metal complexes that feature closely spaced intraligand $^3\pi,\pi^*$ and ^{3}MLCT levels has it been found that when the intraligand $^3\pi,\pi^*$ state is lowest in energy, well-resolved vibronic structure is observed in the emission spectrum.[15] Thus, taken together, the PL results suggest that at ambient temperature emission arises primarily from an OAE-based $^3\pi,\pi^*$ state in Ir-2, whereas the red-shifted emission observed from Ru-2 and Os-2 arises from a ^{3}MLCT state, where the acceptor "ligand" for the MLCT transition is the bipyridine unit in the OAE.

Assignment of the ambient temperature emission to a ^{3}MLCT state in the case of Ru-2 and Os-2 is also supported by the correlation between the emission energies and the excited-state energies calculated from electrochemical data. The energy of a MLCT state can be computed by an expression of the form, $E_{MLCT} = \Delta E_{1/2} - \beta$, where $\Delta E_{1/2}$ is the difference in the electrochemical half-wave potentials for the metal centered oxidation and the acceptor based reduction, and β is a constant that reflects coulomb and exchange interactions and the reorganization energy in the MLCT state.[14] The values estimated from the relevant electrochemical potentials are listed in Table 1.[12,14,16] Note that there is good agreement between the computed ^{3}MLCT state energies and the observed emission energies for Ru-2 and Os-2.

Additional information concerning the nature of the excited states for the M-OAEs comes from the PL quantum yield and lifetime data (ϕ_{em} and τ_{em}, respectively) compiled in Table 1. First, ϕ_{em} varies in the order Ir-2 $\approx$ Ru-2 $\gg$ Os, and τ_{em} varies significantly across the series in the order Ir-2 > Ru-2 > Os-2. Insight concerning the factors that give rise to these trends comes from the radiative and nonradiative decay rates (k_r and k_{nr}, respectively). For Ru-2 and Os-2 k_r is $\approx 10^4$ s^{-1} and $k_{nr} \geq 10^6$ s^{-1}. These decay parameters are comparable to values observed for a variety of Ru(II) and Os(II) complexes that luminesce from ^{3}MLCT states;[17,18] this correspondence supports assignment of the luminescent state to ^{3}MLCT for Ru-2 and Os-2. The k_{nr} value is larger in Os-2 because this complex has larger spin−orbit coupling and a lower excited-state energy.[18] The k_r and k_{nr} values for Ir-2 are considerably less than for the other metal−OAEs. The significantly decreased decay rate parameters in Ir-2 support assignment of the emitting state to an OAE-$^3\pi,\pi^*$ state.[19] Interestingly, despite the different nature of the emissive excited state in Ru-2 and Ir-2, the ϕ_{em} values for the two complexes are comparable. The relatively high phosphorescence yield for Ir-2 presumably arises because the large spin−orbit coupling induced by the iridium center promotes radiative decay from the OAE-$^3\pi,\pi^*$ state.

To explore the relationship between the photophysics of the metal−OAEs and their EL performance, a series of EL devices

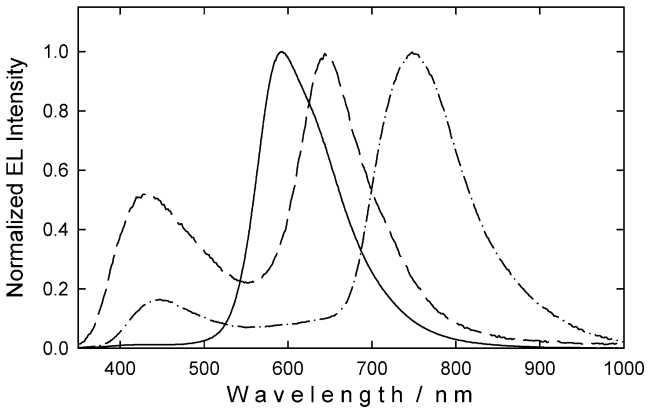

Figure 2. Electroluminescence spectra of devices fabricated with metal−OAE complexes. Device configuration ITO/PEDOT-PSS/PBD: PVK:MOAE/LiF/Al. Legend: (—) Ir-2; (- - -) Ru-2; (—•—) Os-2; Emission band at 450 nm in spectra of Ru-2 and Os-2 arises from the PVK:PBD host.

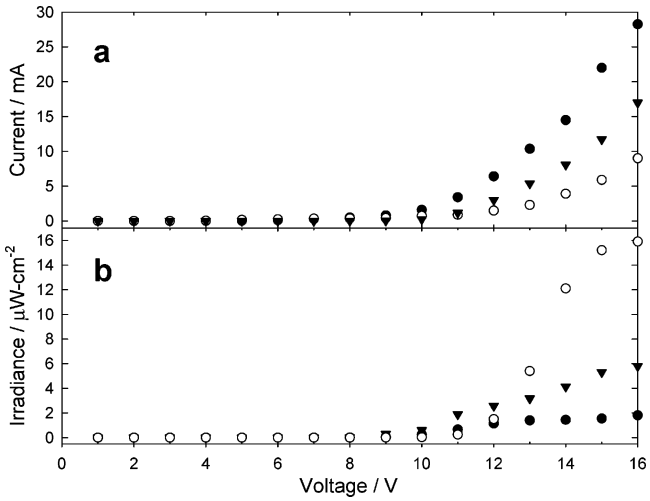

Figure 3. Characteristics of metal−OAE based electroluminescent devices: (a) current−voltage plots; (b) visible irradiance−voltage plots. Device area 0.07 cm^2. Legend: (○) Ir-2; (▼) Ru-2; (●) Os-2.

were fabricated in an identical manner using each of the complexes. Device fabrication and testing methods are described briefly in the Experimental Section, and more details are provided as Supporting Information. Briefly, the anode consisted of $InSnO_2$ (ITO) coated with a thin film of poly(ethylenedioxythiophene):poly(styrenesulfate) (PEDOT-PSS). The active material was a 100 nm spin-coated film consisting of 5 wt % of the metal−OAE complex dispersed in a host matrix containing 47.5 wt % poly(vinylcarbazole) (PVK, a hole-transporting polymer) and 47.5 wt % 2-(4-*tert*-butylphenyl)-5-(4-biphenylyl)-1,3,4-oxadiazole (PBD, an electron transporting material). The cathode consisted of a 0.5 nm layer of LiF topped by a 200 nm aluminum film. A single 2.5 × 2.5 cm ITO substrate featured eight individual 0.07 cm^{-2} electroluminescent device "elements", each of which could be individually characterized. The data presented herein represents the average of data obtained on at least two substrates with 8 devices.

Electroluminescence spectra obtained at a bias of 11 V for three typical metal−OAE based devices are shown in Figure 2. Red EL is observed from devices fabricated using each of the metal−OAEs and the EL band maxima (Table 1) correlate closely with the PL λ_{max} values obtained for the corresponding complexes in the MTHF glass at 80 K.[20] This correlation is expected because the PVK:PBD matrix is rigid like the MTHF solvent glass. In addition, the correlation between the EL and PL band maxima for the metal−OAEs suggests that for each complex the EL emanates from the same excited state that is responsible for the PL emission (i.e., ^{3}MLCT for Ru-2 and Os-2 and $^3\pi,\pi^*$ for Ir-2). In addition, note that the EL spectrum of the Ir-2 device features little, if any, emission from the PVK host; however, the spectra of the Ru-2 and Os-2 based devices exhibit blue emission from the PVK matrix in addition to the red emission characteristic of the metal−OAE dopants. This observation suggests that energy transfer and/or electron (or hole) transfer from the host to the dopants may be less efficient in the Ru-2 and Os-2 devices.

Figure 3 shows current−voltage and irradiance−voltage plots for the EL devices. All of the devices turn on at approximately 9 V, consistent with previous reports on EL devices that are based on metal−organic dopants in hole transport polymers.[21] The most notable effect is that the Ir-2 based device emits more brightly at lower current density compared to the Ru-2 and Os-2 based devices, indicating that the Ir-2 device operates more efficiently. This is confirmed by experiments in which the peak external EL efficiencies (ϕ_{EL}) were determined (Table 1). Specifically, it can be seen that the Ir-2 device operates with ϕ_{EL} of ≈1%, whereas the QE for EL from the Ru-2 and Os-2 devices is approximately 5- and 30-fold lower, respectively. Note that although the EL efficiencies for the metal−organic devices are modest compared to those seen for optimized devices based on evaporated films of organometallic Ir(III) complexes,[3] in general they are considerably higher than efficiencies typically observed for single layer devices that contain conjugated organic oligomers. In these systems, EL emanates from the singlet manifold, and efficiencies in the range of 10^{-3} to 10^{-4} are typical.[22−25]

The relatively low PL QE of Os-2 is the primary reason that the Os-2 based device features the lowest EL efficiency. However, given that the PL QEs are similar for Ir-2 and Ru-2, it is surprising that EL efficiency of the Ir-2 based devices is so much larger. In previous investigations that examined ϕ_{EL} for OLEDs based on series of metal-complex emitters with the same type of excited state, it was observed that there is a direct correlation between the ϕ_{EL} and ϕ_{PL}.[3] In view of this, the finding that the efficiency of the Ru-2 based device is lower than that of the Ir-2 device is of interest. Although a definitive explanation for this issue is not possible on the basis of the EL work carried out to date, it is possible to posit factors that may contribute to the lower ϕ_{EL} for the Ru-2 devices. First, due to the higher ionic charge on Ru-2 (Ru-2 is a dication, and Ir-2 is a monocation), this metal−OAE may not disperse as well in the PVK:PBD matrix. Aggregation of the metal−OAE may decrease the efficiency of energy and/or charge transfer from the host to the Ru-2 dopant. A second and more interesting possibility is that the improved efficiency of the Ir-2 based device is correlated with the fact that this complex features an OAE $^3\pi,\pi^*$ lowest excited state. This factor may be important, because it is possible that if e^-/h^+ recombination occurs on the OAE, then in the Ir-2 based devices the luminescent OAE $^3\pi,\pi^*$ state is directly produced by recombination with high efficiency (due to the favorable spin-statistics for triplet production).[4] By contrast, in the Ru-2 based devices if e^-/h^+ recombination occurs on the OAE producing the $^3\pi,\pi^*$ state, an internal conversion step (i.e., $^3\pi,\pi^*$ to ^{3}MLCT) is required prior to EL light emission, and this additional step may result in lost efficiency. Further investigations are in progress to investigate the origin of the difference in ϕ_{EL} for the Ru-2 and Ir-2 devices.

In summary, we have investigated the photophysics and electroluminescence properties of a series of d^6 metal complexes

of an aryleneethynylene oligomer "ligand". The photophysical results indicate that the Ru(II) and Os(II) systems feature lowest ^{3}MLCT excited states, whereas the Ir(III) complex features an oligomer-based $^3\pi,\pi^*$ lowest excited state. All three complexes exhibit red EL at wavelengths corresponding with the PL observed from the complexes in a rigid solvent glass. Characterization of the EL device performance demonstrates that the Ir-2 devices operate with considerably higher efficiency compared to the Ru-2 and Os-2 based devices. The higher efficiency of the Ir-2 device may be related to the $^3\pi,\pi^*$ nature of the emissive excited state.

Experimental Section

Ru-2, Ir-2, and Os-2 were prepared as described previously.[12,26] PBD (Acros) and PVK (Aldrich, M_w 1 100 000) were used as purchased. Absorption spectra were measured on a double-beam Cary-100 UV−visible spectrometer. Visible photoluminescence spectra were recorded using a Fluorolog-2 fluorescence spectrophotometer (ISA-Spex). The Fluorolog was equipped with a thermoelectrically cooled Hamamatsu R-928 PMT detector, and the emission spectra were corrected for the instrument response using correction factors generated in-house with a primary standard lamp. Photoluminescence spectra of Os-2 were measured on a home-built fluorescence spectrometer that is equipped with a Triax 180 spectrograph (ISA-Spex) equipped with a liquid N_2 cooled silicon CCD detector (ISA-Spex, EEV CCD chip, 1024 × 128 pixels). The Triax-CCD spectrometer has a nearly flat spectral response from 400 to 1000 nm. Low-temperature photoluminescence spectroscopy was carried out with samples contained in a Liquid N_2 optical cryostat (DN-1704, Oxford Instruments, LTD).

Electroluminescent devices were prepared by masking and then etching the ITO coated glass (Delta Technologies, R_s = 8−12 Ω) by exposure to aqua regia vapor. Following etching, the ITO glass substrate was sequentially cleaned by sonication in aqueous sodium dodecyl sulfate (SDS) (Fisher), Milli-Q water, acetone, and 2-propanol. The ITO glass was then dried under a stream of N_2. A hole-transport layer of PEDOT-PSS (Bayer Baytron P VP Al 4083) was spin-coated onto the ITO surface at 4000 rpm and subsequently dried in a vacuum oven at 150 °C for 4 h. Solutions in $CHCl_3$ containing 5 wt % metal−OAE complex and 1:1 PBD:PVK were then spin-coated onto the substrate. The resulting films were dried under vacuum (1×10^{-6} Torr) for 12 h at room temperature. Lithium fluoride and aluminum layers were sequentially deposited by thermal evaporation at 4×10^{-7} Torr without breaking vacuum between depositions. The thicknesses of the deposited LiF and Al layers were determined to be 5 and 2000 Å, respectively, using a calibrated oscillating quartz crystal thickness monitor. After deposition, the devices were encapsulated with epoxy (Loctite quick-set epoxy). Electroluminescence spectra were recorded on the Triax-CCD spectrometer. Power for the electroluminescence device measurements was supplied using a Keithley 2400 voltage−current source. A primary standard tungsten lamp was used to calibrate the Triax-CCD spectrometer in irradiance units (μW cm^{-2} nm^{-1}), and external quantum efficiencies were calculated as described in the literature.[27]

Acknowledgment. We gratefully acknowledge the National Science Foundation (CHE-0211252) for support of this work. G.B.C. is an Alumni Research Fellow at the University of Florida.

Supporting Information Available: Detailed description of the methods used to fabricate and test the light emitting devices (9 pages). This information is available free via the Internet at http://pubs.acs.org.

References and Notes

(1) Baldo, M. A.; O'Brien, D. F.; You, Y.; Shoustikov, A.; Sibley, S.; Thompson, M. E.; Forrest, S. R. *Nature* **1998**, *395*, 151−154.

(2) Adachi, C.; Baldo, M. A.; Thompson, M. E.; Forrest, S. R. *J. Appl. Phys.* **2001**, *90*, 5048−5051.

(3) Lamansky, S.; Djurovich, P.; Murphy, D.; Abdel-Razzaq, F.; Lee, H. E.; Adachi, C.; Burrows, P. E.; Forrest, S. R.; Thompson, M. E. *J. Am. Chem. Soc.* **2001**, *123*, 4304−4312.

(4) Wilson, J. S.; Dhoot, A. S.; Seeley, A. J. A. B.; Khan, M. S.; Köhler, A.; Friend, R. H. *Nature* **2001**, *413*, 828−831.

(5) Handy, E. S.; Pal, A. J.; Rubner, M. F. *J. Am. Chem. Soc.* **1999**, *121*, 3525−3528.

(6) Carlson, B.; Phelan, G. D.; Kaminsky, W.; Dalton, L.; Jiang, X.; Liu, S.; Jen, A. K. Y. *J. Am. Chem. Soc.* **2002**, *124*, 14162−14172.

(7) McDonagh, A. M.; Bayly, S. R.; Riley, D. J.; Ward, M. D.; McCleverty, J. A.; Cowin, M. A.; Morgan, C. N.; Varrazza, R.; Penty, R. V.; White, I. H. *Chem. Mater.* **2000**, *12*, 2523−2524.

(8) Hagfeldt, A.; Grätzel, M. *Acc. Chem. Res.* **2000**, *33*, 269−277.

(9) Peng, Z. H.; Gharavi, A. R.; Yu, L. P. *J. Am. Chem. Soc.* **1997**, *119*, 4622−4632.

(10) Walters, K. A.; Ley, K. D.; Cavalaheiro, C. S. P.; Miller, S. E.; Gosztola, D.; Wasielewski, M. R.; Bussandri, A. P.; van Willigen, H.; Schanze, K. S. *J. Am. Chem. Soc.* **2001**, *123*, 8329−8342.

(11) Li, Y.; Whittle, C. E.; Walters, K. A.; Ley, K. D.; Schanze, K. S. In *Electronic, Optical and Optoelectronic Polymers and Oligomers*; Jabbour, G. E., Meijer, E. W., Sariciftci, N. S., Swager, T. M., Eds.; Materials Research Society: Warrendale, PA, 2002; Vol. 665, pp 61−72.

(12) Glusac, K. D.; Jiang, S.; Schanze, K. S. *Chem. Commun.* **2002**, 2504−2505.

(13) Kober, E. M.; Meyer, T. J. *Inorg. Chem.* **1983**, *22*, 1614−1616.

(14) Vlcek, A. A.; Dodsworth, E. S.; Pietro, W. J.; Lever, A. B. P. *Inorg. Chem.* **1995**, *34*, 1906−1913.

(15) Ohsawa, Y.; Sprouse, S.; King, K. A.; DeArmond, M. K.; Hanck, K. W.; Watts, R. J. *J. Phys. Chem.* **1987**, *91*, 1047−1054.

(16) $E_{1/2}^{ox}$ values (potentials in V vs SCE): Ir-2, +1.40 quasi-reversible; Ru-2, +1.37; Os-2, +0.93. $E_{1/2}^{red}$ values: Ir-2, −0.92; Ru-2, −0.91; Os-2, −0.92.

(17) Barqawi, K. R.; Murtaza, Z.; Meyer, T. J. *J. Phys. Chem.* **1991**, *95*, 47−50.

(18) Kober, E. M.; Caspar, J. V.; Lumpkin, R. S.; Meyer, T. J. *J. Phys. Chem.* **1986**, *90*, 3722−3734.

(19) Baba, A. I.; Shaw, J. R.; Simon, J. A.; Thummel, R. P.; Schmehl, R. H. *Coord. Chem. Rev.* **1998**, *171*, 43−59.

(20) PL spectra and quantum efficiencies were also determined for the complexes in the PVK/PBD EL matrix. The PL maxima and relative quantum yields observed for the matrix dispersed materials are as follows. Ir-2: $\lambda_{max}^{PL} = 597$ nm, $\phi_{PL} = 0.011$; Ru-2, $\lambda_{max}^{PL} = 654$ nm, $\phi_{PL} = 0.016$; Os-2: $\lambda_{max}^{PL} = 790$ nm, $\phi_{PL} < 0.001$.

(21) Chen, F.-C.; Yang, Y.; Thompson, M. E.; Kido, J. *Appl. Phys. Lett.* **2002**, *80*, 2308−2310.

(22) Gebhardt, V.; Bacher, A.; Thelakkat, M.; Stalmach, U.; Meier, H.; Schmidt, H. W.; Haarer, D. *Adv. Mater.* **1999**, *11*, 119−123.

(23) Robinson, M. R.; Wang, S. J.; Bazan, G. C.; Cao, Y. *Adv. Mater.* **2000**, *12*, 1701−1704.

(24) Arias-Marin, E.; Arnault, J. C.; Guillon, D.; Maillou, T.; Le Moigne, J.; Geffroy, B.; Nunzi, J. M. *Langmuir* **2000**, *16*, 4309−4318.

(25) Maillou, T.; Le Moigne, J.; Geffroy, B.; Lorin, A.; Rosilio, A.; Dumarcher, V.; Rocha, L.; Denis, C.; Fiorini, C.; Nunzi, J. M. *Synth. Met.* **2001**, *124*, 87−89.

(26) Ley, K. D.; Li, Y. T.; Johnson, J. V.; Powell, D. H.; Schanze, K. S. *Chem. Commun.* **1999**, 1749−1750.

(27) He, Y.; Hattori, R.; Kanicki, J. *Rev. Sci. Instrum.* **2000**, *71*, 2104−2107.

(28) Caspar, J. V. Ph.D. Dissertation, University of North Carolina, Chapel Hill, NC, 1982.

(29) Kober, E. M.; Marshall, J. L.; Dressick, W. J.; Sullivan, B. P.; Caspar, J. V.; Meyer, T. J. *Inorg. Chem.* **1985**, *24*, 2755−2763.